ACADEMIC RESEARCHES IN ENGINEERING SCIENCES

Editor
Assoc. Prof. Özdoğan KARAÇALI, Ph.D.

DUVAR

ACADEMIC RESEARCHES IN ENGINEERING SCIENCES

Editor

Assoc. Prof. Özdoğan KARAÇALI, Ph.D.

Academic Researches in Engineering Sciences
Editor: Assoc. Prof. Özdoğan KARAÇALI, Ph.D.

Editor in Chief: Berkan Balpetek
Cover and Page Design: Duvar Design
Printing : First Edition-October 2020
Publisher Certificate No: 16122
ISBN: 978-625-7767-75-0

853 Sokak No:13 P.10 Kemeraltı-Konak/Izmir/ Turkey
Phone: 0 232 484 88 68
www.duvaryayinlari.com
duvarkitabevi@gmail.com
Printing and Binding: Sonçağ Yayıncılık Matbaacılık Reklam San. Ve Tic. Ltd. İstanbul Cad. İstanbullu Çarşısı No:48/48-49
İskitler 06070 Ankara/Turkey
Phone: 03123413667
Certificate No:47865

CONTENTS

Chapter-1

Advanced Biomaterial Premolar Dental Implants: Structural Analysis of the Biomechanical Behavior on The Maximum Von-Mises Stress Deformation Response By Three-Dimensional Finite Element and Topology Optimization Method

Özdoğan KARAÇALI[*] *, Ph.D.*

[*] Department of Mechanical Engineering, Faculty of Engineering, Istanbul University-Cerrahpaşa, Avcılar, Istanbul, Turkey

ABSTRACT

Topology optimization increases the resistance or natural frequency while reducing the weight by regulating the distribution of the elements within the design volume within the determined constraints. In last two decades, many efforts have been made to optimize the shape of different type products by topology optimization method. There is few research on the subject of topology optimization of the shape of dental implants in registered literature. The purpose of this study applied topology optimization as a new approach in finite element method to search for unnecessary material distribution on a dental threaded implant and redesign a new implant macrogeometry of abutments with the evaluation of its biomechanical functions.

The purpose of this research is to generate evaluations between deformation and von Mises stress citeria occured tooth roots in the direction of analysis by FEA and biomechanical topology optimization method. In this work, related studies about stresses on the new dental implant and their effects have been investigated for biomaterial. The selection of bioceramic materials for bone implant is covered with a default maximum stresses and strains studied regions. Failure of the implant fracture for dental implants are still critical to study stresses and deformations on the dental implant. Also stresses that occur between the implant and bone were examined. As a result, the condition of the biomaterial implant in terms of the jawbone, the structure of the jaw of the stretch fractures, and the prevention of subsequent fractures are extremely important to do biomechanical topological optimisation in this analysis. The analysis software ANSYS Workbench LS-DYNA v19.0 was used and modeled at the SolidWorks 2019. The virtual analysis showed promising results to design better and stronger implant dentals by topology optimization approach.

Keywords: Dental implants, premolar implant, computational design, finite element method, stress analysis, bioceramic materials, topology optimisation

1 INTRODUCTION

For centuries, man has developed various methods to replace lost teeth for functional and aesthetic reasons. One of these methods is to repair toothless spaces with an implant [1]. Implants, literally, they are inanimate substances placed in the body and living tissues for the purpose of treatment and function[2]. Dental implants, on the other hand, are structures that are placed inside the bone, on the mucosa and intended to replace the tooth [3]. The aim of implants is to provide a direct functional and structural association between the dental implant system and healthy and living bone tissue, ie osseointegration [4].

The word implant consists of a combination of latin words, which means planting, placing. The process of ensuring aesthetic and functional continuity by placing biocompatible materials and appliances in or on the bone is called oral implantology [5]

Dental implants are placed into the jaw- bone to perform the functions of lost teeth, and they are artificial tooth roots. The implants in the jawbone, with a specific surface are placed in a minor surgical operation. To fulfill the functions of lost teeth, dental implants are much more widespread in recent times [6]. There are various models of different brands in the market. In addition implant materials, add to the diversity of brands and models [7,8]. The selection of material as the crutial factor [10], is the biomechanical properties [8]. Considering that one of the reasons for failure of the implant fracture [11, 12], dental implants are still important to study stresses on the implant [13,14, 15]. A type-specific implant consists of a titanium screw with a rough or smooth surface, the outer surface of which resembles a tooth root [16]. The vast majority of dental implants consist of commercially pure titanium [17, 18]. Implant surfaces are treated by plasma spraying [19], anodizing [20], acidic etching [21]and

sandblasting [22] which enlarge the surface area and increase its integration potential [23].

Biological material titanium is acceptable for bone and the most suitable metal for dental implants [24]. It is also used in plaques and screws applied in some fractures in the medical field [25]. It is one of the most resistant metals. Since it is accepted by the human organism, there is no fear of rejection by the body [26, 27]. Per-Ingvar Brånemark [28, 29, 30] worked with titanium, and some current research has focused on the use of ceramic materials such as Zirconia (ZrO2) in implants [31, 32, 33]. The purpose of this research was to analyze mechanical properties of dental implants. By applying engineering tools such as the finite element method (FEM) and von Mises analysis, it was investigated how dental implant devices withstand chewing power during chewing cycles. Molar dental implant and original tooth structure are shown in Figure 1. The next section will explain materials and methods for premolar dental implant.

Coming sections will explain topology optimization algorithm development for dental implants, modeling methods of computer aided process implants, mechanical analysis and topology optimization applied to material optimization of abutment in dental implant.

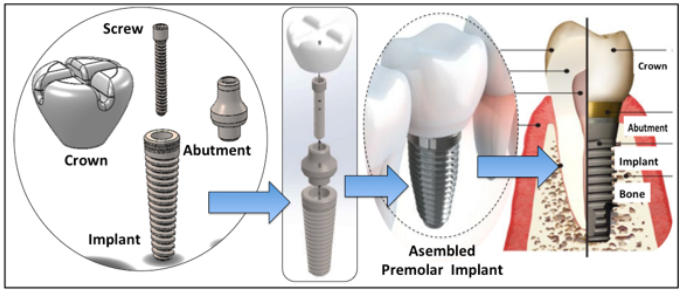

Figure 1. Molar dental implant and original tooth structure

2 ADVANCED DENTAL IMPLANT BIOMATERIALS

When biomaterials are placed inside the body, they react with the tissue. Materials such as carbon, pyrolytic carbon, vitreous carbon, ceramics can be considered as materials that have been and are still in use in modern implantology. Today, titanium and titanium alloys are the most commonly used materials in the construction of implants.

Metallic biomaterials are materials that best adapt to mechanical conditions in the musculoskeletal system. Metallic biomaterials are durable structures that do not lose their properties against heavy, long-term, variable and sudden loading at certain limits. Metals and metal alloys, which have superior mechanical properties due to their crystal structure and strong metallic bonds, have a large share in the biomaterial field. On the one hand, it is used as joint prosthesis and bone renewal material in orthopedic applications, es well as artificial heart parts, catheters, valves, heart valves in facial and maxillofacial surgery, such as dental implants or cardiovascular surgery.

Although ceramics tend to exhibit high strength, hard, brittle, chemically inert (corrosion resistance) insulating behavior in terms of electrical and thermal properties, they exhibit a wide variety of properties. The ceramics are used as biomaterials and being biocompatible is that they contain ions in the body (zirconium, titanium). Oxide Ceramics are polycrystalline ceramics that are inert and formed as a result of the dispersion of metal ions in the plane formed by oxygen ions. These materials are used as bone powder in orthopedic veneers and dental implants, facial bones, ear bones, hip and knee prostheses. This calcium phosphate-based ceramic, which is one of the bioceramics, is used as artificial bone in the construction of various prostheses, repair of cracked and broken bones and coating of metallic biomaterials. In this research, bioceramic implant materials behaviour was studied with a maximum stresses and strains as given in the next sections.

3 MATERIALS AND METHODS

The tensions caused by the bite force in the jaw structure, which is modeled in three dimensions, were investigated in this section. The strength of the molar dental implant, dental crown, abutment, and bone tissue interacting with the implant was investigated at the end of the analysis. The reason for investigating the stresses and deformations is to measure the durability of the implant system. At the same time, the reason for the analysis of the stresses between the implant and the bone is to determine how much force the bone is forced while applying the bite force on the molar dental implant. This analysis has been carefully considered since the prosthesis will fail if the implant causes deformation on the bone when it forces the bone.

The bite burden load of the human is taken as a load. It is considered as a chewing and bite force. This corresponds to a range from 200N to 500N in an adult male. In the examination of the stresses on the bone, forces were applied using the 3D model commercial ANSYS Workbench v20. created in SolidWorks 2019 software. All models were imported into ANSYS for meshing and stress analysis. The material values of elasticity module and poisson coefficient that define the physical properties of the models used in study are shown in Table 1 in accordance with the literature. In order to provide a more realistic simulation, cortical and trabeculous bone is assumed to be anisotropic, homogeneous and linear elastic. All other materials are accepted as isotropic, homogeneous and linear elastic. Titanium and Ceramic Porcelain Properties are summuriesed in Table 1.

In the results of the analysis, the bolt made of pure titanium material has taken into account the yield strength for the abutments and implants and the breaking strength for other models. In mechanical models, Von-Mises equivalent stress result was evaluated for yield

strength, and maximum prime stress results were compared to yield strength.

Table 1. Titanium and Ceramic Porcelain Properties

	Young Module (GPa)	Poison ratio	Yield Strength (MPa)	Tensile Strength (MPa)
Pure Titanium (Ti-55)	105	0.37	377	440
Ceramic Porselain	22059	0.22	-	172

The research in this paper explained, consists of four stages. In the first stage, research and data related to dental bone and dental implants were provided, the material for the implant was pure titanium (Ti-55), and the ceramic porcelain material was chosen for the original rooted model. The data obtained in the second stage are drawn in Solidworks environment and 3D modeling is done. In the third stage; Analyses of the selected part was made using 3D models. The topology optimization method was applied to molar dental implant system in stage four. Next section explains all these research steps by finite element analysis of molar implant.

4 FINITE ELEMENT ANALYSIS OF MOLAR IMPLANT

It is very difficult and costly to carry out stress analysis under living tissues in dental region [35]. Therefore, it is more convenient to do biomechanical evaluation on a lifeless simulation model in ANSYS [36]. Three-dimensional models obtained by computer aided design method were taken into ANSYS environment for analysis. Static Structural ANSYS was chosen from the analysis modules of the program for evaluation. Meshed implant and forces applied to molar dental system are shown in Figure 2.

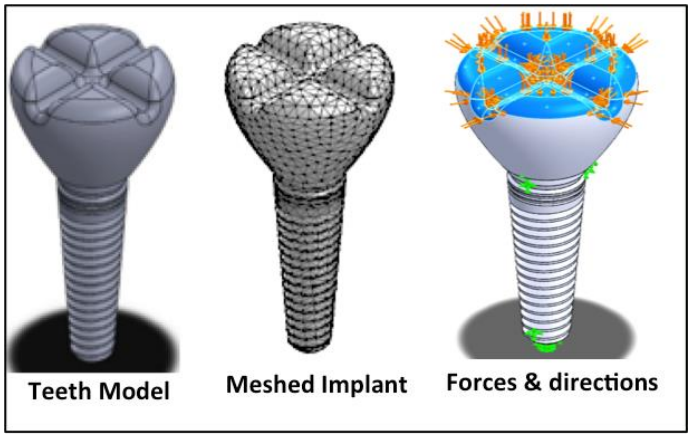

Figure 2. Meshed implant and forces applied

The implants to be used in the study were modeled as 3.5 mm in diameter, 9 mm in length, with a cylindirical structure and internal connection, following the standard design principles. It has been assumed that the osseointegration of the implants in the models with the jaw bone is 100%. Abutment heights are modeled as 5 mm in cement design and 2 mm in screw design. Implants and abutments are connected by screws. On the abutments, the first mandibular first molar tooth ceramic crown design was simply modeled and the region corresponding to the distal triangular fossa where the occlusal force will be applied was determined to be in the same region in both types of crowns.

FEA is a computer-based numerical solution method that allows examination of internal and external stress, compression stress and displacements occurring under loads applied to complex geometry structures [37]. Finite element method is frequently used in various fields of dentistry such as implant dentistry and is applied in a wide variety of simulations [38]. Although it is used as a useful tool to predict the stress effect on the material and biomaterial under the forces applied today, it has some

limitations. Therefore, both the modeling and analysis stages should be checked with great care. In this comparative study, the finite element method was chosen for stress analysis. It is not an interventional process; it is a numerical technique that allows analyzing internal and external stresses, strains and displacements in any area of the structure under study. Since the patterns, stresses and displacements in the areas of prosthetic implant bone complex, which cannot be accessed by other biomechanical study methods, cannot be identified; the finite element method was employed by performing the abutment application with the tpology optimization described in the last section of this study.

5 Analysis of Molar Implant

Premolars are the broad, flat teeth located at the back of the mouth before the molar teeth. When eating, premolars help crush, grind, and mash food so it's easier to swallow. In this study, maximum and minimum principal strain values of premolar in the cortical and trabecular bone and von Mises strain values in the premolar implants were investigated together with images showing stress distributions as shown in Figure 2. The von Mises stress is used to determine the tensile strength of retractable materials. It also determines the onset of deformation of retractable materials. Implants are retractable materials and this value is 550 MPa. In this study, maximum and minimum principal stress values occurring in cortical and trabecular bone and von Mises stress values occurring in implants have been examined together with images showing stress distributions as shown in Figure 3. The von Mises stress is used to determine the tensile strength of retractable materials. It also determines the onset of deformation of retractable materials. Implants are retractable materials and this value is 550 MPa. When the von Mises stress values exceed this, the von Mises stress values will fail.

In order to make analysis on mathematical models, the surface relationships of the parts that make up the model must be defined in the program. It is assumed that the jaw bone, implant, abutment, zirconium substructure and crown, that is, implant and superstructure materials are in continuous contact. Implants are assumed to be 100% osseointegrated to the jaw bone.

The models are made up of four-node tetrahedron elements as much as possible. In areas close to the center of the structures in the models, the mesh density has been increased to make the structure more suitable for analysis when necessary. In order to facilitate the calculation through this modeling technique, it has been tried to create the highest quality network structure with the most suitable node elements. Steep and narrow regions in the jaw models that make the analysis process difficult, have been made more orderly. For the study to give realistic results, the most suitable number of elements has been tried to be reached by considering the dimensions of the jaw bone model we have chosen, as far as the ANSYS program allows.

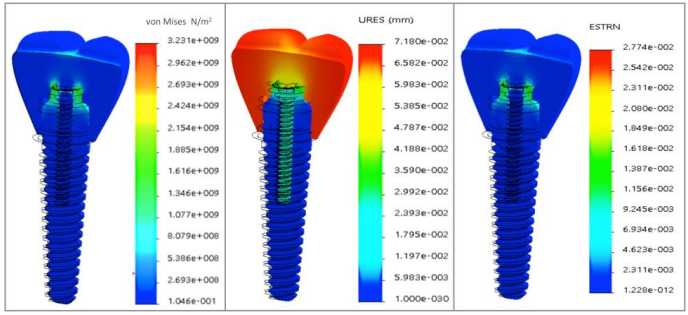

Figure 3. Premolar implant analysis

As a result of finite element analysis, von Mises stresses and displacements in the implant, flat and angled abutment, zirconium substructure, crown and mandible were investigated. Von Mises stress is considered as a composite stress value, and Von Mises stress values give

an idea of the distribution of stresses in the structure of fragile materials. Von Mises stress and displacement results were recorded as colored images. In these images, each color defines a range of values; the range of values is shown by the scale on the side of the images. This study evaluates the influence of commercially available dental implant systems on stress distribution in the prosthesis, abutment, implant, and supporting alveolar bone under simulated occlusal forces, employing a finite element analysis. The implants and abutments evaluated consisted of a stepped cylinder implant connected to a screw-retained, internal, and a conical implant connected to a solid, internal, conical abutment. A porcelain covered, silver-palladium alloy was used as a crown. In each case, a simulated, 200-N vertical load was applied to the buccal cusp. A finite element model was created based on the physical properties of each component, and the values of the von Mises stresses generated in the abutment, implant, and supporting alveolar bone were calculated.

In the implant, the maximum von Mises stresses were concentrated at the points of load application in both systems, and they were greater in abutment (150 N/mm^2). Within the limits of this investigation, the stepped cylinder implant connected to a screw-retained, internal conical abutment produces greater stresses on the alveolar bone and prosthesis and lower stresses on the abutment complex. In contrast, the conical implant connected to a solid, internal, conical abutment furnishes lower stresses on the alveolar bone and prosthesis and greater stresses on the abutment. Implant displacement URES (mm) and nodal stress calculation are shown in Figure 4 and Figure 5.

The scientists stated that implant breaks occurred during use as a result of fatigue rather than excessive loads [1, 30, 34]. Stress buildup in a dental implant to prevent fatigue fracture. It is necessary to use materials with a suitable design and high fatigue resistance or

increased by certain processes. Measures that can be taken at the design stage, according to the type of implant; It is especially aimed at preventing micro mobility between the abutment and the implant body and increasing the moment load that the implant can carry [35].

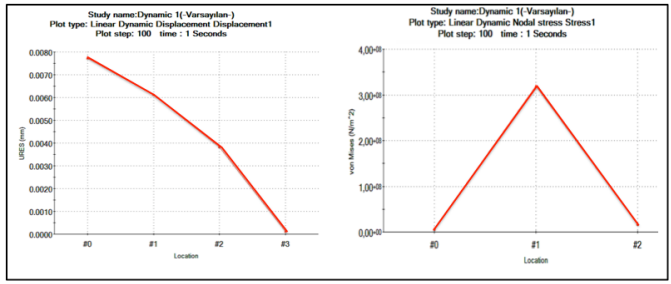

Figure 4. Implant displacement URES (mm) and nodal stress

At this step fatigue analysis starts. The loading frequency is selected as 15 Hz, and the constant amplitude load option is R = σmin / σmax = 0.1, completely reversed. Mean stress correction theory for equivalent von Mises criteria has been selected in fatigue life solutions. The Fatigue analysis resolves the problem regarding to the von Mises stress criteria in the nodes obtained from the static analysis.

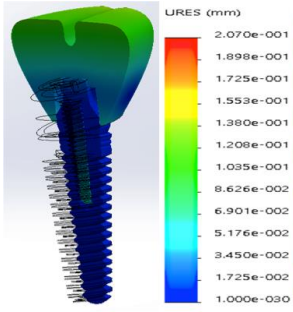

Mass Participation (Normalized)

Mode Number	Frequency(Hertz)	X direction	Y direction	Z direction
1	5345.4	9.8408e-005	5.477e-011	2.0752e-006
2	5806.4	0.0044762	8.8245e-006	0.26216
3	5819.1	0.26385	1.9179e-007	0.0045141
4	9076.1	0.0005993	5.755e-009	0.0086703
5	9160.7	0.0083858	7.7582e-010	0.0080409
6	17643	0.038538	6.6275e-005	0.47397
7	17703	0.47217	2.3166e-008	0.038514
8	27769	3.6581e-006	0.79299	2.0288e-005
9	52933	0.0011781	2.9277e-007	0.00074381
10	53157	0.00069141	5.4189e-007	0.0011675
11	66304	3.0249e-007	8.2313e-007	1.0237e-007
12	79926	7.8299e-007	9.3363e-008	2.254e-008
13	80524	6.0211e-007	3.8952e-007	1.8393e-008
14	1.1308e+005	8.4242e-006	0.013162	8.2065e-010
15	1.2059e+005	1.4852e-008	0.0012312	5.1037e-008
		Sum X = 0.798	Sum Y = 0.80746	Sum Z = 0.79783

Figure 5. The displacement with different frequencies [Hz]

6 TOPOPLOGY OPTIMIZATION OF DENTAL IMPLANT

Designers are based on their experience and similar designs made before designing. The designs obtained in this way are mostly not the most efficient design and the design needs to be improved. For this reason, designers need optimization studies after the basic design they create [38].

Optimization is the optimization study of a problem within the design constraints and goal function by changing the design variables. One of the most used optimization techniques structurally is topology optimization as shown in Figure 8. Evolving computer technology and processor powers have contributed to the development and further use of topology optimization.

Topology optimization increases the resistance or natural frequency while reducing the weight by regulating the distribution of the elements within the design volume within the determined constraints. In topology optimization, two different methods, homogenization method and density method, are used to determine the distribution of the elements [39]. Topological optimization theory tries to minimize the structural adjustment energy called objective function [40, 41]. This use is necessary for the standard option problem minimum volume (V) of topological optimization. Configuration about topology optimization problem:

Objective function (Uc) (1)

$0 < \eta_i < 1$ (i=1,2, 3,…, n) limitations (2)

$V \leq V_o - V^*$ (3)

$V = \sum_i \eta_i V_i$ (4)

$E_i = E(\eta_i)$ (5)

$\{\sigma_i\} = [E_i]\{\varepsilon_i\}$ (6)

U_c is the energy of structural fulfillment, V is the computed volume, V_0 is original and V* is the material amount to be removed, E is the elasticity tensor, σ_i is the stress ε_i is strain where η_i is the pseudodensities interconnected to each finite element (i) in the topology optimisatiom method. The finite element analysis used in this study, solves optimization problems using the density method, also known as material distribution. In the material distribution method, a temporary material density is the design variable and is therefore often referred to as the density method. The material density varies between 0 and 1, 0 represents the state to be emptied and 1 the state where there will be no discharge. The method uses the following expression to describe the change in density between 0 and 1 between stiffness and density [40].

Topology optimization consists of a series of processes from the creation of the first design to the optimum design. First of all, designers create the first design considering their working conditions, connection points and strength conditions within their knowledge and experience as shown in Figure 2. Then analyse strain stresses, displacement and static energy az shown in Figure 3. After the displacement with different frequencies [Hz] as demonstarted in Figure 5, all data

related to mechanical stress analysis, then topology optimization can be applied. The first step in topology optimization is to create the design volume through the design created by the designers with their own experience. On the design volume, the areas where unloading is desired and topology optimization will not be applied are determined.

The finite element model of the design, which is divided into zones where unloading is desired and unloading is not created. Boundary conditions in the working conditions of the part are applied to the finite element model. The durability requirements and purpose expected from the design are determined as the goal function and design constraints for topology optimization and topology optimization is run. As a result of abutment optimization in dental implant system, element densities are displayed depending on optimization constraints and objective function. The optimum shape is redesigned over the element densities by considering production constraints. On the created design, the conditions determined for the design are applied again and it is examined whether the optimum shape meets the conditions. According to the findings mentioned in early sections in the analysis of Von Mises stress values in this study, maximum stress loading was observed in the implant abutments. Thus, the abutment was analysed by finite element analysis using topology optimization. The topology optimization for abutment in dental implant system is as shown in Figure 6.

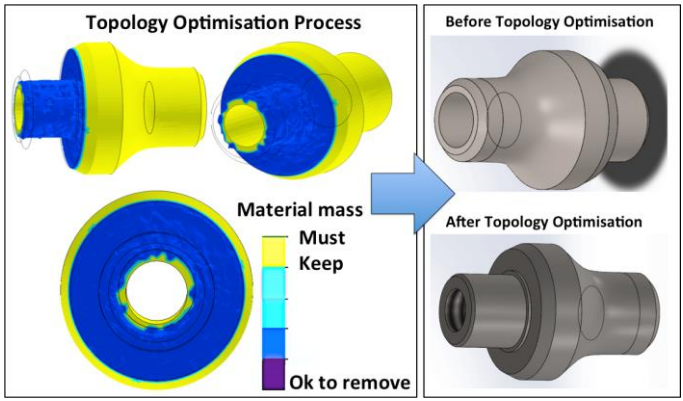

Figure 6. Topology optimization for abutment

This study result shows “it is okay to remove” and “must keep” warning for the redesign. For this analysis top of the abutment needs to be thinner. In order to make the best design of the part, structural analysis and data acquisition are provided in the computer environment. For the dental implant designed in this study, a comparison was made according to abutment materials.

First, 3D modeled parts were assembled in Solidworks. Based on two materials compared for the best dental implant design, a new design was obtained with topology optimization.

7 Results and Discussions

For the dental implant abutment, such a complicated shape structure as shown in Figure 6, with high resolution comprehensive for the density area topology optimization is difficult. The finite element approach for the stiffness of thin-walled structures should be used with caution, as it may not be true that the structure is only one element wide [38, 39, 40]. This is in various parts of the solution. The topology optimization of the abutment in the implant section is a shape optimization based on the

results of this study, where the results can increase confidence in the results.

For the optimization design of the abutment of the dental implant, it is necessary to make use of strain energy resulting from the static forces and the maximum weight of the structure by comparing it with the original design as shown in Figure 7. In this way, optimization gives results that show the same displacement and weight as the original design as shown in Figure 8. New design of abutment strength was increased from 30 MPa (shown in Figure 3) to maximum von Mises value 80 MPa as demonstrated in Figure 9.

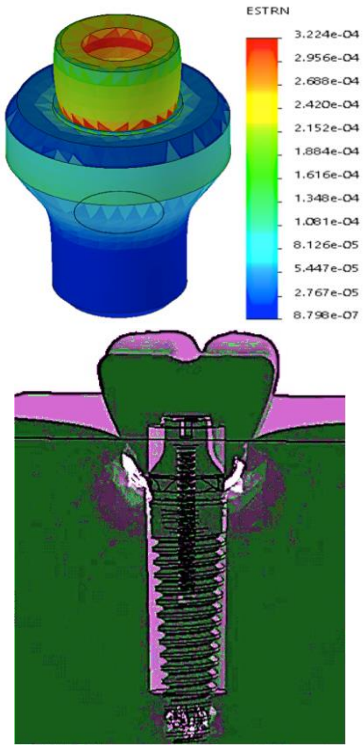

Figure 7. Equivalent strain ESTRN analysis

Equivalent strain of abutment is the apparent change in the shape in dental implant, volume or length of object caused due to stress is called strain. Equivalent strain ESTRN analysis topology optimization shown in Figure 7.

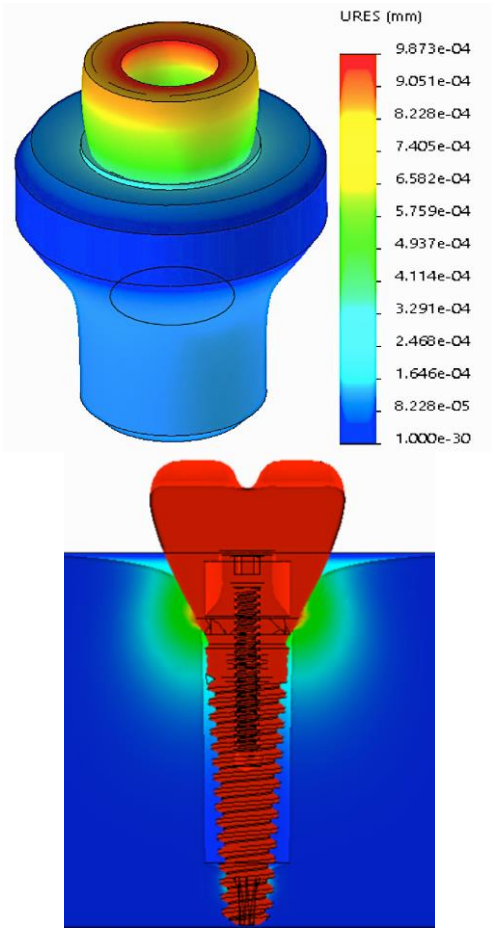

Figure 8. Displacement analysis for abutment in dental implant system

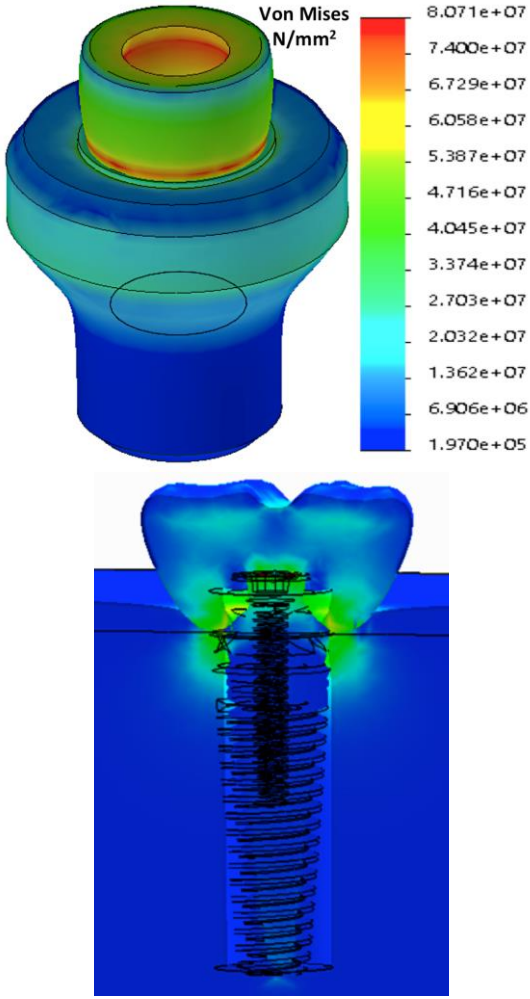

Figure 9. The von Mises criteria for abutment after topology optimization

8 CONCLUSIONS

The von Mises and deformation analysis of premolar dental implantwas realised by using software ANSYS Workbench LS-DYNA v19.0 and modeled at the SolidWorks 2019. The virtual analysis showed promising results to design better and stronger implant dentals by topology optimization approach.

This research found out that the type of loading is biomechanical stress on dental implant and abutment. Topology optimization was used to analyze and improve the abutment design that is part of the dental implant. It contains special importance to the static and dynamic behavior of the abutment, which is in the dental implant structure. Optimized results have been shown to perform better than the original design. In real life, when using implant premolar teeth, it should be observed whether implant performance improves and more research is needed. Comparing Von Mises stress criteria, better results have been achieved with topology optimization. When we examine it as data, it is seen that the stress values that the material of the abutment can meet is higher than the original design. With the new implant abutment topology optimization, the volume and material density are evaluated, reducing the volume of the traditional implant by approximately 12%. Until the implant, the implant abutment was able to meet the stiffness of the ceramic crown and bone complex.

9 REFERENCES

1. Karaçalı, Ö. (2015). Material Fatigue Research for Zirconia Ceramic Dental Implant: a Comparative Laboratory and Simulation Study in Dentistry. *Acta Physica Polonica A*, 127 (4): 1195-1198.

2. Karaçalı, Ö. (2014). A Research on Structured Analysis of Biomaterial of Dental Implant in Computer Aided Biomechanical Engineering Modeling. *Acta Physica Polonica A*, 125 (2): 186-188.
3. Quaresma , S. E. T., Cury, P. R., Sendyk W. R., Sendyk C. (2008). Finite Element Analysis of Two Different Dental Implants: Stress Distribution in the Prosthesis, Abutment, Implant, and Supporting Bone. *Journal of Oral Implantology* XXXIV(1): 122-140.
4. Silva G. C., (2019). Biomechanical evaluation of screw- and cement-retained implant-supported prostheses: A nonlinear finite element analysis. *The J. of Prosthetic Dentistry*, 112 (6): 28-39.
5. Lemos, C. A. A., (2018). Splinted and Nonsplinted Crowns with Different Implant Lengths in the Posterior Maxilla by Three-Dimensional Finite Element Analysis. *Journal of Healthcare Engineering*, 18 (1): 1-7.
6. Pellizzer, E. P., Mello C. C., Santiago J. F., de Souza B. V. E., Almeida D. A. F., and Verri F. R., (2015) Analysis of the biomechanical behavior of short implants: the photo-elasticity method. *Materials Science Engineering C Mater Biological Applications*, 55: 187–192.
7. Goiato, M. C., dos Santos D. M., Santiago J. F., Moreno A., and Pellizzer, E. P. (2014). Longevity of dental implants in type IV bone: a systematic review. *International Journal of Oral and Maxillofacial Surgery*, 43(9): 1108–1116.
8. Pellizzer, E. P., Lemos, C. A. A., Almeida, D. A. F., de Souza B. V. E., Santiago J. F., and Verri F. R., (2018). Biomechanical analysis of different implant-abutments interfaces in different bone types: an in silico analysis. *Materials Science*

Engineering C Mater Biological Applications, 90(1): 645–650.
9. Pessoa R. S., Sousa R. M., Pereira L. M. et al., (2017). Bone remodeling around implants with external hexagon and morse-taper connections: a randomized, controlled, split- mouth, clinical trial. *Clinical Implant Dentistry and Re- lated Research*, (19)1: 97–110.
10. Kumar H., Verma M., Lamba A. K., Faraz F., Kirti R., (2011). Restoration of maxillary anterior defect using autogenous block graft and optimizing the esthetics using zirconia restoration. *International Journal of Oral Implantology and Clinical Research*, 2(3): 165-170
11. Smeets R., Stadlinger B., Schwarz F., Beck-Broichsitter B., (2016). Impact of dental implant surface modifications on osseointegration. *BioMed Research International*, 2016(1): 23-40.
12. Gore E., Evlioglu G., (2014). Assessment of the effect of two occlusal concepts for implant-supported fixed prostheses by finite element analysis in patients with bruxism. *Journal of Oral Implantology*, XL(1): 67-90.
13. Cicciù, M., Cervino, G., Milone, D., Risitano, G. (2018). FEM investigation of the stress distribution over mandibular bone due to screwed overdenture positioned on dental implants, *Materials*, 12(11): 1512-1530.
14. Bevilacqua, M., Tealdo, T., Pera, F., (2008). Three-dimensional finite element analysis of load transmission using different implant inclinations and cantilever lengths. *Int J Prosthodont*, 21:539– 542.
15. Lemos C. A., Ferro-Alves M. L., Okamoto R., M. R. Mendonca, and Pellizzer E. P., (2016). Short dental implants versus standard dental

implants placed in the posterior jaws: a systematic review and meta-analysis. *Journal of Dentistry*, 47: 8–17.
16. Lemos C. A. A., Verri F. R., Santiago Ju´nior J. F., (2018). “Retention system and splinting on morse taper implants in the posterior maxilla by 3D finite element analysis,” Brazilian Dental Journal, vol. 29, no. 1, pp. 30–35,
17. J. F. Santiago Junior, F. R. Verri, D. A. Almeida, V. E. de Souza Batista, C. A. Lemos, and E. P. Pellizzer, “Finite element analysis on influence of implant surface treatments, connection and bone types,” Materials Science Engineering C Mater Biological Applications, vol. 63, pp. 292–300, 2016.
18. C. A. Lemos, V. E. Souza Batista, D. A. Almeida, J. F. Santiago Junior, F. R. Verri, and E. P. Pellizzer, “Evaluation of cement-retained versus screw-retained implant-supported restorations for marginal bone loss: a systematic review and meta-analysis,” Journal of Prosthetic Dentistry, vol. 115, no. 4, pp. 419–427, 2016.
19. Abu-Hammad A, Harrison A, Williams D, The effect of a hydroxyapatite-reinforced polyethylene stress distributor in a dental implant on compressive stress levels in surrounding bone, Int J Oral Maxillofac Implants, 2000, 15:559–564.
20. Brånemark, P.I., Hansson, B.O., Adell, R., Breine, U., Lindström, J., Hallén, O., Ohman, A., (1997). Osseointegrated implants in the treatment of the edentulous jaw - experience from a 10-year period. *Scand. J. Plast. Reconstr. Surg.* 16: 1–132.
21. B Reham. O., S. Michael V., (2015). A Critical Review of Dental Implant Materials with an Emphasis on Titanium versus Zirconia, *Materials*, 8: 932-958.

22. Cicciù M., Cervino G., Milone D., Risitano G., (2019). Fem analysis of dental implant-abutment interface overdenture components and parametric evaluation of equator and locator prosthodontics attachments, *Materials*,12: 592-612.
23. Cervino, G., Romeo, U., Lauritano, F., Bramanti, E., Fiorillo, L., D'Amico, C., Milone, D., Laino, L., Campolongo, F., Rapisarda, S., et al. (2018). FEM and von Mises analysis of osstem® dental implant structural components: evaluation of different direction dynamic loads. *Open Dent. J*., 12: 219–229
24. Bramanti, E., Cervino, G., Lauritano, F., Fiorillo, L., D'Amico, C., Sambataro, S., Denaro, D., Famà, F., Ierardo, G., et al., (2017). FEM and von mises analysis on prosthetic crowns structural elements: Evaluation of different applied materials. *Sci. World J.*, 12: 34-50
25. Lauritano, F., Runci, M., Cervino, G., Fiorillo, L., Bramanti, E., Cicciù, M., (2016). Three-dimensional evaluation of different prosthesis retention systems using finite element analysis and the Von Mises stress test. *Minerva Stomatol*, 65: 353–367.
26. Karl, M., (2009). Biomechanical methods applied in dentistry: a comparative overview of photoelastic examinations, strain gauge measurements, finite ele ment. *Eur J Prosthodont Restor Dent*isyry,17:50–57.
27. Castilla, R., (2019). Comparative study of the influence of dental implant design on the stress and strain distribution using the finite element method. *Journal of Physics: Conf. Series* 11(59): 120-160.
28. Macedo J. P., Pereira J., Faria J., Pereira C. A., Alves J. L., Henriques B., Souza J C M (2017). Finite element analysis of stress extent at peri-implant bone surrounding external hexagon or

morse taper implants. *J. Mech. Behav. Biomed. Mater*., 71: 441–447.
29. Meirelles L., Brånemark P. I., Albrektsson T., Feng C., Johansson C., (2019). Histological evaluation of bone formation adjacent to dental implants with a novel apical chamber design: preliminary data in the rabbit model Clin. *Implant Dent. Relat. Res.* 17: 453–460.
30. Udomsawat C, Rungsiyakull P, Rungsiyakull C, Khongkhunthian P., (2019). Comparative study of stress characteristics in surrounding bone during insertion of dental implants of three different thread designs: A three- dimensional dynamic finite element study. *Clin. Exp. Dent. Res.* 5:26–37.
31. Shirazi, H., Ayatollahi, M. R., Karimi, A., (2016). A comparative finite element analysis of two types of axial and radial functionally graded dental implants with titanium one around implant-bone interface. *Science and Engineering of Composite Materials*, 24(5): 747–754.
32. Razaghi, R., Biglari, H., Karimi, A., (2017). Dynamic finite element simula- tion of dental prostheses during chewing using muscle equivalent force and trajectory approaches. *Journal of Medical Engineering & Technology*. 41:314–324.
33. Oftadeh, R., Perez-Viloria, M., Villa-Camacho, J. C., (2015). Biomechanics and mechanobiology of trabecular bone: a review. *Journal of Biomechanical Engineering*. 137: 0108021–01080215.
34. Jianhua A, Li T., Liu Y., Ding Y., Wu G., Hu K. , Kong L., (2010). Optimal design of thread height and width on an immediately loaded cylinder implant: A finite element analysis.

Computers in Biology and Medicine 40: 681–686.
35. T. Ohyama, S. Nakabayashi and H. Yasuda et al., (2019). Mechanical analysis of the effects of implant position and abutment height on implant-assisted removable partial dentures, *Journal of Prosthodontic Research.* 9: 7-17.
36. Marimuthu V. K., Kumar K., Sadhasivam N., Arasappan R., (2015). Finite element analysis of stress and displacement around mini-implant using different insertion angles and various direction of orthodontic force in maxilla and mandible. *J Indian Orthod Soc*, 49:61-6.
37. Kim J. J., Jang I. G., (2016). Image resolution enhancement for healthy weight-bearing bones based on topology optimization. *Journal of Biomechanics.* 49: 3035–3040.
38. Chang C.-L., (2012). Finite element analysis of the dental implant using a topology optimization method. *Medical Eng. & Physics* 34: 999–1008.
39. Bendsoe, M. P., Sigmund, O., (2014). Topology optimization, theory, methods, and applications. Springer Verlag, NY.
40. Ghaheri A., Shoar S., Naderan M., Hoseini S. S., (2015). Genetic Algorithms in Medicine. *Oman Medical Journal,* 30(6): 406–416.

Chapter-2

Durability Characteristics Of Lightweight Concretes Obtained With Polyester Coated Pumice Aggregates

İzzet Çelik[*]
Alper Bideci[**]
Bekir Çomak[***]
Özlem Sallı Bideci[****]
Batuhan Aykanat[*****]

* Düzce University, Graduate School of Natural and Applied Sciences, Department of Civil Engineering, 81600,

** Düzce University, Faculty of Art, Design and Architecture, Department of Architecture 81600, Düzce

*** Düzce University Faculty of Technology, Department of Civil Engineering 81600, Düzce

**** Düzce University, Faculty of Art, Design and Architecture, Department of Architecture 81600, Düzce

***** Düzce University Faculty of Technology, Department of Civil Engineering 81600, Düzce

ABSTRACT

Following the developments in the area of constructional materials, studies on lightweight concretes produced with coated aggregates have increased. In this study, pumice aggregates were coated with bulk polyester to obtain coated aggregates. Granulometry, specific weight, loose unit weight and water absorption tests were performed on coated aggregates. Also, lightweight concretes with polyester coated aggregate (PCP) and control concrete samples (NCP) with 400 kg/m^3 and 500 kg/m^3 dosages were produced. On the manufactured concrete samples, not only physical and mechanical tests but also accelerated sulphate tests were performed in order to determine the effects of chemical environments. In this study, for all batches of NCP and PCP concrete samples with 400 kg/m^3 and 500 kg/m^3 dosages which were tested after 2,7 and 28 days, it was observed that concrete compressive strength values increased with time. Concrete samples of NCP-400 were determined to be in the strength class of LC 25/28, whereas NCP-500, PCP-400 and PCP-500 were determined to be in the strength class of LC 30/33. When concrete samples obtained with polyester coated aggregates were analysed, it was found that water absorption and splitting tensile strength values decreased in PCP batches compared to NCP batches, and according to ultrasonic pulse velocity values all concrete samples fell into "good quality" concrete classification. In the accelerated sulphate (Na_2SO_4 and $MgSO_4$) test (20 cycles), it was observed that loss of mass of PCP samples were less than that of NCP samples. As a result of the study, it was determined that with coating polyester on pumice aggregates, water absorption values for the concrete was decreased and by this special aggregates, structural lightweight concretes resistant to sulphate effects could be produced.

Keywords: *Concrete, Polyester Coated, Pumice, Durability, Strength*

1 Introduction

Pumice is a type of igneous rock formed as a result of volcanic events, and it is spongy, porous, glassy and resistant to physical and chemical effects. During formation of pumice, many numbers of pores are formed as the gases inside leave the body immediately and it suddenly cools down. Pumice is used as an industrial raw material or an additive in more than fifty sectors throughout the world [1]. Within the constructon industry it is especially preferred due to its resistance to combustion or fire, its potential to decrease the amount of energy consumed and its insulation properties [2]. Advantages of pumice aggregate in the production of lightweight concretes compared with normal aggregate can be listed as follows; it decreases dead load due to its low density, provides high heat and sound insulation, plasters would readily adhere to it, it has good acoustic properties and it is fire resistant. However, the high water absorption capacity of lightweight aggregates due to their porous structure creates a disadvantage in lightweight concrete production [3, 4]. To avoid disadvantages of pumice aggregates the investigators have produced coated lightweight aggregates with enhanced physcial and chemical properties by using mineral or chemical additives and different coating methods. There are studies determining physical, mechanical and durability characteristics of lightweight concretes obtained by using these coated lightweight aggregates. Sallı Bideci et al. (2015) have determined that for lightweight concretes produced by coating grinded colemanite on pumice aggregate, cement + colemanite coating had positive contribution to rapid chlorine permability values [5], there were experienced less damage from high temperature effect due to this coating [6] and the adherence performance of lightweight concretes had improved with the reinforcement [7] . Bideci et al. (2013) have determined that coated aggregates have increased compressive strength values in lightweight concretes and when polyurethane and polyester coated pumice aggregates

were compared, it was found that polyester coated pumice aggregates had more porous structure than polyurethane coated aggregates, and polyurethane coated aggregates could be used in the production of lightweight concretes (500 kg/m^3 dosage) [8]. It was determined that concretes produced with polymer coated aggregates could be used in unpressurised aqueous environments and carried less corrosion risk, [9] and this also positively effected its stretching and shrinking characteristics. [10] .

Getting damaged due to a chemical attack is a serious problem which affects strength and robustness of concretes. Main chemical attacks are acid and sulphate attacks. Therefore, protective measures to decrease the chemical attacks to the concretes have great importance. Bideci (2013), investigated the durability characteristics of lightweight concretes produced with colemanite coated lightweight aggregates. The study was performed on samples kept in 5% Na2SO4 and MgSO4 solutions for 28, 90 and 365 days. As a result of the study, it was concluded that samples kept in MgSO4 solution were less damaged and their durability characteristics were better than the samples kept in Na2SO4 solution.[2].

In this study, to obtain coated aggregate, pumice aggregate with 16 mm of maximum grain diameter was coated with bulk polyester. Four different batches of concrete samples (PCP-400, PCP-500, NCP-400 and NCP-500) were produced by using CEM-I 42,5 R (400 kg/m^3 and 500 kg/m^3 dosages) cement with polyester coated and non-coated pumice aggregate and natural sand. Within this concept, unit weight and flow tests were applied on fresh concrete samples, while dry unit weight, compressive strength, splitting tensile strength, water absorption, ultrasonic pulse velocity and accelerated sulphate effect tests were applied on hardened concrete samples in accordance with related standards.

2. Material and Method

Natural sand in 0/4 mm mesh size as fine aggregate, pumice aggregates in 4/8 mm and 8/16 mm mesh size, polyester as aggregate coating material, marble powder as a material to prevent adherence of aggregates to each other were used in the study.

2.1 Material

Two different kinds of aggregates as non-coated natural sand (0-4 mm) and polyester coated pumice aggregate (4-8, 8-16mm) were used. Pumice aggregate was obtained from the mine belonging to Metaş Madencilik Ltd. Şti located in Nevşehir city Merkez district Çardak village. CEM I 42.5/R cement produced in accordance with TS EN 197-1 is used as the binder[11] and marble powder obtained from the market is used to seperate the aggregates from each other during coating them with polyester. Chemical analysis of mineral based chemicals used are given in Table 1.

Table 1. Chemical analysis of mineral based materials used (%)

Chemical Composition	SiO_2	Al_2O_3	Fe_2O_3	CaO	MgO	K_2O	Na_2O	SO_3	Loss of Ignition
Pumice	74.10	13.45	1.40	1.17	0.35	4.10	3.70	-	1.54
CEM I 42,5/R	19.70	5.25	3.46	62.85	1.27	-	0.29	3.35	2.14
Marble Powder	-	-	0.02	31.16	23.31	0.01	0.51	-	44.89

Polyester used during the study is a bulk, unsaturated polyester resin. With its good filling and low shrinking capacity, besides its usage in applications like casting with filling, it is also possible to use it in applications that do not require rapid curing and high thermal resistance. Technical properties of the material are given in Table 2 [12].

Table 2. Technical Properties of Polyester

Material Structure	Test Method	Bitumen Modified Polyester
Tensile Strength	ISO 0527	66 MPa
Elongation at break, Tensile	ISO 0178	2.50%
Elongation at break, Bending	ISO 0178	5.94%
Flexural Strength	ISO 0178	138 MPa
Water Absorption	ISO 0062	0.16%
Colour	max. 100 Hazen	
Density in liquid	1.125 g/cm^3	

2.2 Coating of Pumice Aggregates with Polyester

Coating was applied on 4-8 mm and 8-16 mm aggregate grain groups. Aggregates were coated by spraying polyester with a conventional type paint gun. As a result of preliminary studies, polyester which could not be sprayed by the paint gun due to its high concsistency was thinned by adding cellulosic thinner in a ratio of 8% by weight. To cover the aggregate surface completely and obtain sufficient coating thickness, coating was applied as it would be three layers. To seperate the aggregates that adhere to each other during polyester coating, marble powder is applied on them. Coated aggregates were dried at 23±2 ºC temperature for 96 hours on average. Non-Polyester Coated and Polyester Coated Pumice Aggregates are shown in Figure 1.

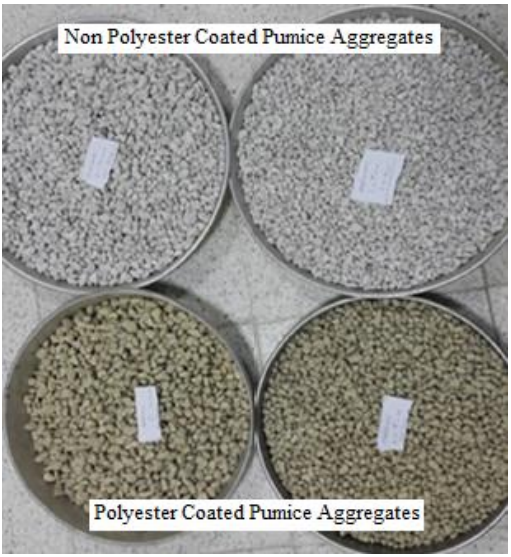

Figure 1. Non-Polyester Coated and Coated Pumice Aggregates

2.3 Method

Granulometry, specific weight, loose unit weight and water absorption tests were performed on non-polyester coated and coated aggregates in the study. Also, lightweight concrete samples with polyester coated pumice aggregates (PCP) and with non-polyester coated pumice aggregates (NCP) were produced in 400 kg/m^3 and 500 kg/m^3 dosages and they were compared. On the manufactured concrete samples, not only physical and mechanical tests, but also accelerated sulphate tests were performed in order to determine the effects of chemical environments.

2.3.1 Aggregate tests

Pumice Aggregates were dried in an oven for 24 hours at 60ºC. Sieve analysis on oven-dried aggregates was performed in accordance with TS EN 933–1 [13] standard. Against the possibility of a size change in aggregates coated with polyester, sieve anlaysis was repeated after

coating. In aggregate tests, the specific weight test result was found by displacement of water by volume for coated and non-coated pumice aggregates. Loose unit weight test was performed in accordance with TS EN 1097-3 [14] and water absorption ratio test was performed in accordance with TS EN 1097-6 [15].

2.3.2 Fresh concrete tests

To determine the processability of the fresh concrete, consistency test with slump method was applied in accordance with TS EN 12350–2 [16] and unit weight test was applied in accordance with TS EN 12350-6 [17] standard.

2.3.3 Hardened concrete tests

On cubic concrete samples in the size of 100×100×100 mm obtained by Non-Polyester Coated Pumice Aggregates (NCP) and Polyester Coated Pumice Aggregates (PCP), unit weight test and water absorption test were performed in accordance with TS EN 12390-7 [18] standard and compressive strength test (after 2, 7 and 28 days) was performed in accordance with TS EN 12390-3 [19] standard. Splitting tensile strength test was applied in accordance with TS EN 12390–6 standard [20] and ultrasonic pulse velocity test was applied according to ASTM C 597 standard [21] on cylinder samples of 100×200 mm size.

Accelerated sulphate test was performed with two different solutions as Sodium Sulphate (Na_2SO_4) and Magnesium Sulphate ($MgSO_4$). 28 pieces of NCP and PCP concrete samples produced in 100x100x100 mm sizes were dried in an oven at 60 ˚C for 2 days after 28 days of cure period. For the test, Na_2SO_4 and $MgSO_4$ in solid form were dissolved in pure warm water as they would be 1.17% and 1.29% by weight, respectively. After oven dried weights of prepared lightweight concrete samples were determined, they were placed in Na_2SO_4 and $MgSO_4$ solutions. Solutions were mixed for a certain time and they retained

their homogenity. Samples were exposed to sulphate environment by keeping them in Na_2SO_4 solution for 12 hours and in $MgSO_4$ solution for 24 hours. After that, the samples were taken out of the solutions and rinsed with clean water. Samples exposed to Na2SO4 were dried for 12 hours while samples exposed to MgSO4 were dried for 24 hours in an oven at 105 ˚C. Samples taken from the oven were reweighed. All these processes are called as "one cycle" and samples were exposed to sulphate environment for 20 cycles.

3. Design of Concrete Mixture

In the study, non-polyester coated and coated lightweight aggregate samples were used and 400 kg/m^3 and 500 kg/m^3 dosages of light concrete test batches were prepared. Air content of these mixtures were accepted as 3%. 1 m^3 mixture design of eact test batch is given in Table 3.

Table 3. Concrete mixing ratios (1m^3)

Components		**400 kg/m^3 Dosage**		**500 kg/m^3 Dosage**	
		NCP-400	**PCP-400**	**NCP-500**	**PCP-500**
Aggregate Mesh Size (mm)	**8 – 16 (kg)**	92	131	92	131
	4 – 8 (kg)	150	225	150	225
	0 – 4 (kg)	1006	1006	1006	1006
Water (kg)		241	207	208	180
Cement (kg)		400	400	500	500

4. Results and Discussion

4.1 Aggregate Test Results

According to grain size distribution test result, aggregates used in the study were found to be in accordance with TS 706 EN 12620 [22] standard. Specific weight, loose unit weight and water absorption ratio results of non-polyester coated and coated aggregate samples are given in Table 4.

Table 4. Specific Weight, Loose Unit Weight and Water Absorption Ratio Results of Non-Polyester Coated and Coated Aggregates

Mixtures	Specific Weight (g/cm^3)			Loose Unit Weight (kg/m^3)			Water Absorption Ratio (%)		
	0 – 4	4 - 8	8 - 16	0 – 4	4 – 8	8 - 16	0 – 4	4 – 8	8 - 16
NCP	2.67	1.02	0.94	1750	440	390	1.50	19.8	25.2
PCP	-	1.35	1.18	-	635	595	-	1.35	1.95

Specific weight of sand (0-4 mm mesh size) used in the lightweight concrete mixture is 2.67 g/cm^3. As can be seen from Table 4, specific weights of aggregates were between 0.94–2.67 g/cm^3. It was determined that specific weight values of PCP aggregates increased compared to that of NCP aggregates, however they remained below the minimum aggregate specific weight value given in litearture (2.1g/cm^3).

Loose unit volume weight values of aggregates found in accordance with TS EN 1097-3 [14] are given in Table 4. Sand with 0-4 mm mesh size without polymer coating was found to have 1750 kg/m^3 loose unit weight. It was determined that loose unit weight was between 440-635 kg/m^3 for aggregates having 4-8 mm mesh size while it was between 390-595 kg/m^3 for aggregates having 8-16 mm mesh size. According to the obtained results, non-polyester coated pumice aggregates having 4/8 mm and 8/16 mm mesh size were not within 480–880 kg/m^3 as specified in the literature[23], and it was determined that loose unit

weight of pumice increased with polyester coating and thus remained within the range specified in the literature. Also with the increase of specific weight of aggregates coated with polyester it was observed that their loose unit weight also increased naturally.

When water absorption test results were analysed, for non-polyester coated pumice aggregates, water absorption ratio was found as 20% for aggregates with 4-8mm mesh size and about 25% for aggregates with 8-16 mm mesh size. It was determined that water absorption ratio of coated pumice aggregates was 1.35% for aggregates having 4-8 mm mesh size and 1.65% for aggregates having 8-16 mmm mesh size. Water absorption ratios of aggregates after polyester coating has decreased 93% for aggregates with 4-8 mm mesh size and 92% for aggregates with 8–16 mm mesh size. Also, it was found that as the grain diamater increases for both non-polyester coated and coated aggregates, water absorption ratio increases, too.

4.2 Fresh Concrete Tests

Results for consistency test performed by slump method, and unit weight values for fresh concretes are given in Table 5.

Table 5. Specific Weight, Loose Unit Weight and Water Absorption Ratio Results of Non-Polyester Coated and Coated Aggregates

Samples	Slump Amount (mm)	Fresh unit weight (kg/m^3)
NCP-400	80	1847
PCP-400	45	1920
NCP-500	60	1890
PCP-500	35	1965

With results obtained by slump test, the flow classification of concrete mixtures were specified in

accordance with TS EN 206-1 as S2 (35-80 mm)[24]. Also, unit weight of prepared fresh concrete samples were found to be between 1847 kg/m³ and 1965 kg/m³. When fresh concrete samples of 500 kg/m^3 dosage were compared with samples of 400 kg/m^3 dosage in respect of unit weights, for NCP samples it was found that there was an increase in unit weight as 2.3%, whereas for PCP samples it was found that there was an increase in unit weight as 2.4%.

4.3 Hardened Concrete Test Results

Unit weight and water absorption ratio values for hardened concrete samples are given in Table 6.

Table 6. Dry unit weight and water absorption ratio of the samples.

Samples	Unit Weight (kg/m³)	Water Absorption (%)
NCP-400	1707	9.52
PCP-400	1780	8.44
NCP-500	1800	7.16
PCP-500	1840	6.64

When unit weights were compared for concrete samples produced with non-polyester coated and coated aggregates, for PCP samples compared to NCP samples it was found that there was an increase in unit weight as 4.28% for samples with 400kg/m^3 dosage, whereas there was an increase in unit weight as 2.22% for samples with 500kg/m^3 dosage, and unit weight values were between 1707-1840 kg/m³. These values were determined to be below the top limit specified for lightweight concretes in literature (2000 kg/m³).

When water absorption test results were analysed it was found that water absorption ratio for NCP samples with 500 kg/m^3 dosage decreased 24.79% compared with that for NCP samples with 400 kg/m^3 dosage, whereas for PCP

samples with 500 kg/m^3 dosage it has decreased 21.33% compared with that for PCP samples with 400 kg/m^3 dosage. According to the obtained result, based on the cement ratio increase the water absorption ratios of lightweight concretes have decreased. Also, water absorption ratio of concrete samples produced with coated aggregates have decreased for both doses.

Compressive strength test results for produced samples tested after 2,7 and 28 days are given in Table 7, and graphical illustration of the test results are given in Figure 3.

Table 7. Compressive strength test results for concrete samples

Samples	Compressive Strength (MPa)		
	2 Days	7 Days	28 Days
NCP-400	19.42	23.46	27.52
PCP-400	20.95	24.77	29.53
NCP-500	23.35	27.76	32.08
PCP-500	25.86	28.93	32.26

Figure 3. Graphical demonstration of compressive strength test results of concrete samples

In Figure 3, it was found that after 2,7 and 28 days, for 400 kg/m^3 dosage samples there were 7.88%, 5.58% and 7.30% increase in compressive strength values, respectively whereas for 500 kg/m^3 dosage samples there were 10.75%, 4.21% and 0.56% increases in compressive strength values, respectively. When compressive strength values for NCP samples and PCP samples were analysed according to their dosages, for all samples it was observed that compressive strength had increased in accordance with the increase in cement dosage weight.

Compressive strength test results for produced test samples after 7 and 28 days are given in Table 8, and graphical illustration of the test results are given in Figure 2.

Table 8. Splitting tensile strength test results for concrete samples.

Samples	Splitting Tensile Strength (MPa)	
	7 Days	28 Days
NCP-400	2.41	2.87
PCP-400	2.26	2.48
NCP-500	2.90	3.01
PCP-500	2.33	2.40

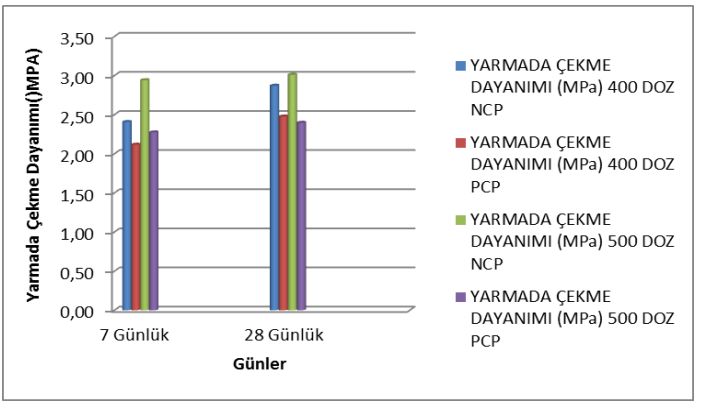

Figure 2. Change in tensile splitting strength test values (MPa).

When 7 days of splitting tensile strength test values of NCP and PCP samples are analysed, it was found that the highest strength value was obtained from NCP-500 samples (2.90MPa) and the lowest value was obtained from PCP-400 samples (2.26MPa). For samples of 28 days, the highest splitting tensile strength was for NCP-500 (3.01MPa) whereas the lowest strength value was for PCP-500 (2.40MPa) samples.

For samples of 500 kg/m^3 dosage compared with

samples of 400kg/m^3 dosage, for NCP samples tested after 7 days and 28 days, it was found that there was an increase as 20.3% and 4.9%, respectively, whereas for PCP samples tested after 7 days there was an increase as 3.10% and for samples after 28 days there was a decrease as 3.20%. It was observed that for NCP samples there was an increase in samples of 7 and 28 days in accordance with the cement dosage increase, whereas in PCP samples there was an increase in samples of 7 days in accordance with the cement dosage increase but splitting tensile strength have decreased in samples of 28 days. Accordingly, it can be concluded that polyester coating of aggregates increased the strength of the aggregate and fracture happened at the weak point which was between concrete and the aggregate surface.

Ultrasonic pulse velocities of produced samples are given in Table 9 and their graphical illustration is given in Figure 3.

Table 9. Ultrasonic pulse velocity test values for concrete samples (km/s).

Samples	Ultrasonic Pulse Velocity (km/h)	
	7 Days	**28 Days**
NCP-400	3.86	3.92
PCP-400	3.89	3.91
NCP-500	3.92	4.08
PCP-500	3.97	3.82

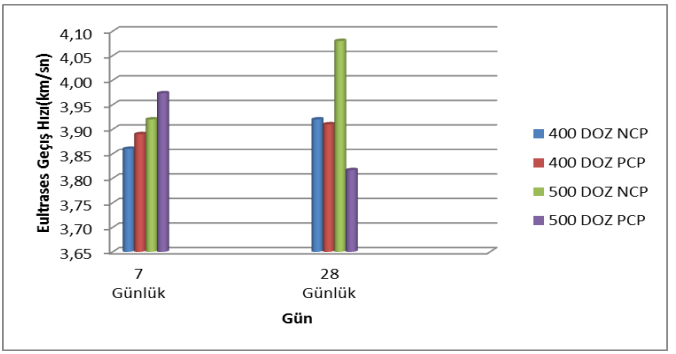

Figure 3. Ultrasonic pulse velocity values for concrete samples (km/h).

It was observed that ultrasonic pulse velocity of the samples produced were between 3.86-4.08 kg/m³. Neville (2013) evaluates "concretes that have ultrasonic pulse velocity more than 4.5 km/h as "excellent", concretes between 3.5-4.5 km/h as "good", those between 3.0-3.5 km/h as "suspected", those between 2.0-3.0 km/h as "bad" and those below 2.0 km/h as "very bad" quality" [3]. When the test results are analysed, it was determined that all samples produced fell into the "good" concrete classification according to literature.

Magnesium Sulphate ($MgSO_4$) and Sodium Sulphate (Na_2SO_4) accelerated sulphate tests were applied on lightweight concrete samples for 20 cycles. As a result of the tests, the percentage of loss of mass for the samples are given in Table 10.

Table 10. Loss of Mass after Accelerated Sulphate Test(%)

Sample	Loss of Mass after 20 Cycles (%)	
	$MgSO_4$	Na_2SO_4
NCP-400	5.9	37.8
PCP-400	3.6	0.5
NCP-500	5.2	0.4
PCP-500	3.9	0.4

When Table 10 is analysed it was found that loss of mass of PCP samples were less than that of NCP samples. When sulphate penetrates into the concrete, it reacts with some components of the cement. As a result of this reaction, it causes deterioration of concrete in time. As a result of the chemical reaction between sulphate ions and components with calcium and aluminium within the hardened concrete, acicular structure (ettringite) and gypsum is formed in the inner structure and as this causes enlargement in the inner structure, cracks, disintegration and loss of mass are observed.

Characteristic appearance of concrete samples after sulphate attack initially looked like white spots that spread to whole area starting particularly from edges and sides which was then followed by formation of cracks and disintegration. Appearance of the sample that was exposed to sulphate attack is given in Figure 4.

Figure 4. Samples that were damaged due to Sulphate effect

As a result of the study, it was determined that by coating aggregates with polyester, the performance of concrete in sulphate environment have increased.

5. Conclusions

Results of tests conducted in this study on lightweight concretes with 400 kg/m^3 and 500 kg/m^3 dosages produced by using non-coated (NCP) and polyester coated (PCP) pumice aggregates are given below, respectively.

Aggregate test results;

- Grain size distribution test performed with normal natural sand aggregate and pumice aggregate were determined to be in accordance with TS 706 EN 12620 standard.
- It was determined that specific weight values of aggregates with 4/8 mm and 8/16mm mesh size increased with polyester coating compared to that of non-coated aggregates, however they remained below the minimum aggregate specific weight value given in literature (2.1g/cm^3).

- It was determined that non-polyester coated pumice aggregates having 4/8 mm and 8/16 mm mesh size were not within 480–880 kg/m^3 as specified in the literature [23], and loose unit weight of pumice increased with polyester coating, and thus remained within the range specified in the literature.
- Water absorption ratio of aggregates after coating with polyester decreased 94% for aggregates with 4-8 mm mesh size and 92% for aggregates with 8–16 mm mesh size. When water absorption ratios of coated and non-coated aggregates were compared with desired water absorption ratios for 24 hours in literature, it was observed that the desired value as 20% with fine aggregates and 30% with coarse aggregates were not exceeded.

Fresh concrete tests;

- Slump values of concrete samples were determined to be between 35-80 mm.
- Unit weights of fresh concretes produced were found to be between 1847 - 1965 kg/m³ . When fresh concrete samples of 500 kg/m^3 dosage were compared with samples of 400 kg/m^3 dosage in respect of unit weights, for NCP samples it was found that there was an increase in unit weight as 2.2%, whereas for PCP samples it was found that there was an increase in unit weight as 2.3%. Therefore, it was determined that concrete unit weight has linear relationship with cement amount.

Hardened concrete tests;

- Unit weight values of PCP and NCP concrete samples were between 1707 - 1840 kg/m³. It was observed that these values did not exceed the top limit (2000 kg/m³) given in literature.
- When water absorption ratios of concrete samples were analysed, it was found that highest water

absorption ratio was for NCP-400 (9.52%), and the lowest water absorption ratio was for PCP-500 (6.64%) samples When compared with NCP samples it was observed that water absorption ratio of PCP samples have decreased 11.34% for 400 kg/m^3 dosage and 7.26% for 500 kg/m^3 dosage. It was determined that water absorption ratio of lightweight concrete samples have decreased by coating of aggregates.

- According to TES EN 2016-1, for concrete samples after 28 days, NCP-400 was determined to be in the strength class of LC 25/28, whereas NCP-500, PCP-400 and PCP-500 were determined to be in the strength class of LC 30/33.
- When splitting tensile strength values were analysed for produced lightweight concrete samples, for samples of 500 kg/m^3 dosage compared with samples of 400kg/m^3 dosage, for NCP samples tested after 7 days and 28 days, it was found that there was an increase as 20.3% and 4.9%, respectively, whereas for PCP samples tested after 7 days there was an increase as 3.10% and for samples after 28 days there was a decrease as 3.20%.
- When the test results were analysed, it was determined that ultrasonic pulse velocity of the samples were between 3.86-4.08 km/h and all produced samples fell into "good" concrete classification.
- Characteristic appearance of concrete samples after sulphate attack initially looked like white spots that spread to whole area starting particularly from edges and sides which was then followed by formation of cracks and disintegration. As a result of the study, it was determined that by coating aggregates with polyester, the performance of concrete in sulphate environment have increased.

As a result of the study, it was shown that a new aggregate and a highly structural special lightweight concrete with decreased water absorption could be

produced by coating pumice aggreates with polyester. Also, heat insulation, chlorine permeability, fire resistance of concrete samples and their interaction with chemical additives used in the concrete can be analysed.

Reference

1. Varol B. Pomza Sektör Raporu (Pumice Sector Report). T C Ahiler Kalkınma Ajansı Nevşehir Yatırım Destek Ofisi 2015:1-12.
2. Bideci ÖS. Investigation of the physical and chemical properties of boron-coated ligthweigth aggregate concrete [Doctoral Thesis]. Edirne, Turkey: Trakya University Institute of Natural Science; 2013.
3. Neville AM. Properties of Concrete PDF eBook: PoC Amazon ePub eBook_o5: Pearson Education; 2013.
4. Rossignolo JA, Agnesini MVC. Mechanical properties of polymer-modified lightweight aggregate concrete. Cement and Concrete Research. 2002;32(3):329-34.
5. Bideci OS, Bideci A, Oymael S, Gultekin AH, Yildirim H. Permeability features of concretes produced with aggregates coated with colemanite. Computers and Concrete. 2015;15(5):883-45.
6. Bideci ÖS. The effect of high temperature on lightweight concretes produced with colemanite coated pumice aggregates. Construction and Building Materials. 2016;113:631-40.
7. Beycioglu A, Arslan ME, Bideci OS, Bideci A, Emiroglu M. Bond behavior of lightweight concretes containing coated pumice aggregate: Hinged beam approach. Computers and Concrete. 2015;16(6):911-20.
8. Bideci A, Gültekin AH, Yıldırım H, Oymael S, Bideci ÖS. Internal structure examination of lightweight concrete produced with polymer-

coated pumice aggregate. Composites Part B: Engineering. 2013;54:439-47.
9. Salli Bideci Ö, Bideci A, Gültekin AH, Oymael S, Yildirim H. Polymer coated pumice aggregates and their properties. Composites Part B: Engineering. 2014;67:239-43.
10. Bideci A, Bideci Özlem S, Oymael S, Yıldırım H. Analysis of shrinkage and creep behaviors in polymer-coated lightweight concretes. Science and Engineering of Composite Materials2014. p. 77.
11. TS EN 197-1. Cement - Part 1: Composition, specifications and conformity criteria for common cements. Turkish Standards Instituion; 2012. p. 1-40.
12. Polipol 3455 Technical Data Sheet. Poliya; 2020.
13. TS EN 933-1. Tests for geometrical properties of aggregates - Part 1: Determination of particle size distribution - Sieving method. Turkish Standards Instituion; 2012. p. 18.
14. TS EN 1097-3. Tests for mechanical and physical properties of aggregates- Part 3: Determination of loose bulk density and voids. Turkish Standards Instituion; 1999. p. 20.
15. TS EN 1097-6. Tests for mechanical and physical properties of aggregates - Part 6: Determination of particle density and water absorption. Turkish Standards Instituion; 2013. p. 51.
16. TS EN 12350-2. Testing fresh concrete - Part 2: Slump test. Ankara: Turkish Standards Instituion; 2010. p. 1-9.
17. TS EN 12350-6. Testing fresh concrete - Part 6: Density Turkish Standards Instituion; 2010. p. 12.

18. TS EN 12390-7. Testing hardened concrete - Part 7: Density of hardened concrete. Turkish Standards Instituion; 2019. p. 11.
19. TS EN 12390-3. Testing hardened concrete - Part 3 : Compressive strength of test specimens. Ankara: Turkish Standards Instituion; 2019. p. 1-19.
20. TS EN 12390-6. Testing hardened concrete - Part 6: Tensile splitting strength of test specimens. Ankara: Turkish Standards Instituion; 2010. p. 1-10.
21. C597-16 A. Standard Test Method for Pulse Velocity Through Concrete. West Conshohocken, PA,: ASTM International; 2016.
22. TS 706 EN 12620+A1. Aggregates for concrete. Turkish Standards Instituion; 2009. p. 50.
23. Chandra S, Berntsson L. Lightweight Aggregate Concrete: Elsevier Science; 2002.
24. TS EN 206:2013+A1. Concrete - Specification, performance, production and conformity. 2017. p. 104.